

Practical emitters for thermophotovoltaics: a review

Reyu Sakakibara^{a,b,*}, Veronika Stelmakh^a, Walker R. Chan^a, Michael Ghebrebrhan^c, John D. Joannopoulos^{a,d}, Marin Soljačić^d, Ivan Čelanović^a

^aInstitute for Soldier Nanotechnologies, Massachusetts Institute of Technology, 77 Massachusetts Avenue, Cambridge, MA 02139, USA

^bDepartment of Electrical Engineering and Computer Science, Massachusetts Institute of Technology, 77 Massachusetts Avenue, Cambridge, MA 02139, USA

^cU.S. Army Natick Soldier Research, Development, and Engineering Center, 15 General Greene Avenue, Natick, Massachusetts, 01760, USA

^dDepartment of Physics, Massachusetts Institute of Technology, 77 Massachusetts Avenue, Cambridge, MA 02139, USA

Abstract. Thermophotovoltaic (TPV) systems are promising for harnessing solar energy, waste heat, and heat from radioisotope decay or fuel combustion. TPV systems work by heating an emitter that emits light that is converted to electricity. One of the key challenges is designing an emitter that not only preferentially emits light in certain wavelength ranges but also simultaneously satisfies other engineering constraints. To elucidate these engineering constraints, we first provide an overview of the state of the art by classifying emitters into three categories based on whether they have been used in prototype system demonstrations, fabricated and measured, or simulated. We then present a systematic approach for assessing emitters. This consists of five metrics: optical performance, ability to scale to large areas, stability at high temperatures, ability to integrate into the system, and cost. Using these metrics, we evaluate and discuss the reported results of emitters used in system demonstrations. Although there are many emitters with good optical performance, more studies on their practical attributes are required, especially for those that are not yet used in prototype systems. This framework can serve as a guide for the development of emitters for long-lasting, high-performance TPV systems.

Keywords: thermophotovoltaic, energy, optics, photonics, light.

*Reyu Sakakibara, reyu@mit.edu

1 Brief introduction to TPV

A thermophotovoltaic (TPV) system converts heat to electricity using light as an intermediary and consists of (at least) three components, which are a heat source, an emitter, and a photovoltaic

(PV) cell with a low bandgap. The heat source brings the emitter to high temperature (≥ 1000 K), causing the emitter to emit thermal radiation, which is absorbed and converted to electricity by the PV cell. Some advantages of this energy conversion scheme include the static and quiet conversion process, the physically separated paths of heat conduction and electricity generation, and the lack of fundamental temperature gradients across materials.¹ In addition, several heat sources can be used, of which there are three major kinds: radioisotope decay, chemical fuel, and sunlight that is concentrated and absorbed (Figure 1). The radiated power density from the TPV emitter is fundamentally limited only by Planck's law for blackbody emission.² However, high-performance TPV systems are particularly challenging to realize in part because of the need to coordinate multiple subsystems and the difficulties in designing a good emitter.

The scope of our review is the TPV emitter, which we consider the critical component towards high system performance, and specifically on its practical implementation in TPV systems. The emitter is any material that is heated up to high temperature. A particularly useful emitter is a selective emitter, which preferentially emits in a specific wavelength region. There is no one way to make an emitter; there are many types of emitters that can each involve a different geometric configuration and a separate set of materials, some of which we touch upon in Section 2.

In our review we propose five metrics to evaluate the practicality of TPV emitters, and in particular we examine emitters that have been used in system demonstrations of TPV prototypes. Most work on TPV emitters has focused on achieving good optical performance, but there has been little consideration of the challenges associated with implementing the emitter in and operating a TPV system.

Our review is organized as follows: in section 2 we classify TPV emitters from the literature into three categories. In section 3 we present and discuss the five metrics for practical TPV emitters

as well as their sub-metrics. In section 4 we provide an at-a-glance evaluation, based on the five metrics, of the five types of emitters used in prototype system demonstrations. The evaluations are summarized in two tables, with one more detailed table in the Appendix (section A).

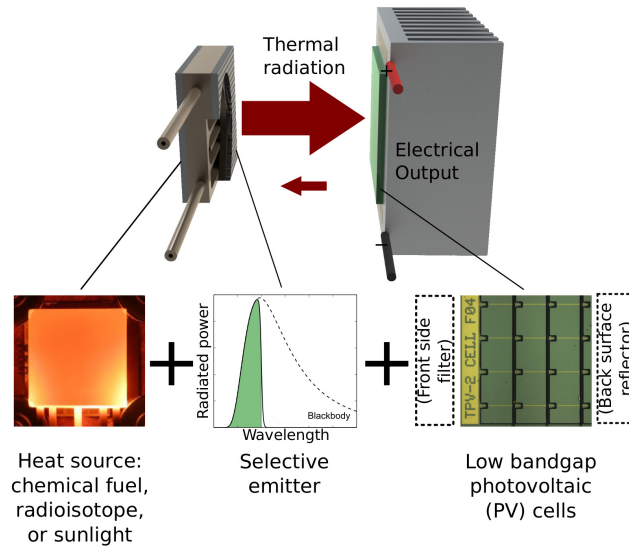


Fig 1 The basic three components of a TPV system are a heat source, an emitter, and a photovoltaic (PV) cell (sometimes the PV cell is known as the TPV cell). The hot side is made up of a heat source in thermal contact with an emitter and converts heat to light. On the cold side, the PV cell converts the thermal radiation from the emitter into electricity. Sometimes the cold side includes a front side filter or back surface reflector, to be explained later. A near-field TPV device has a subwavelength gap between the emitter and the PV cell, but we only focus on standard TPV systems.

2 Classification of TPV emitters

Before evaluating the practicality of TPV emitters, we first classify emitters in the literature into the following categories: i) used in system demonstrations of TPV prototypes ii) fabricated and optical performance measured and iii) optical performance simulated, as shown in Figure 2. In this figure we only include emitters with emission in the range of 1-3 μm , which corresponds approximately to the peak emission wavelengths of typical emitters at temperatures of 1000-1500 K. It is not within the scope of this review to discuss the mechanisms behind different emitters, nor have we provided a complete list of all emitters that have been proposed and fabricated. Detailed discussion of emitter

types, mechanisms, and more examples of emitters can be found in reviews elsewhere, such as that by Pfiester et al.³

Our focus for this review is on the emitters in the first category that have been used for system demonstrations: in section 4, we will evaluate the practical aspects of these emitters, following the discussion of our metrics.

3 Metrics for practical TPV systems

Although the primary purpose to develop an emitter is for its optical performance, the emitter with the best optical performance is not necessarily the best emitter for practical implementation.

For this reason we present five practical metrics, as shown in Figure 3: 1) optical performance 2) ability to scale to large areas 3) long-term high-temperature stability 4) ease of integration within the TPV system and 5) cost.

In the following subsections we will discuss each metric, including some approaches that researchers have taken to address key challenges.

3.1 Optical performance

An emitter with good optical performance has, at all angles, preferential emission of in-band photons and suppression of out-of-band photons. Optical performance refers to the emission of photons as a function of both angle and photon energy, in particular in two regimes for the latter, in-band photons that have energy higher than the PV cell bandgap and out-of-band photons that have energy lower. Spectral control refers to the methods that enable preferential in-band emission. Some designs of spectral control are designed for broadband emission while others for narrow-band emission (the ideal cases which are shown in Figure 4a). In the latter case, the emitted photons have energies

Towards practical emitter implementation

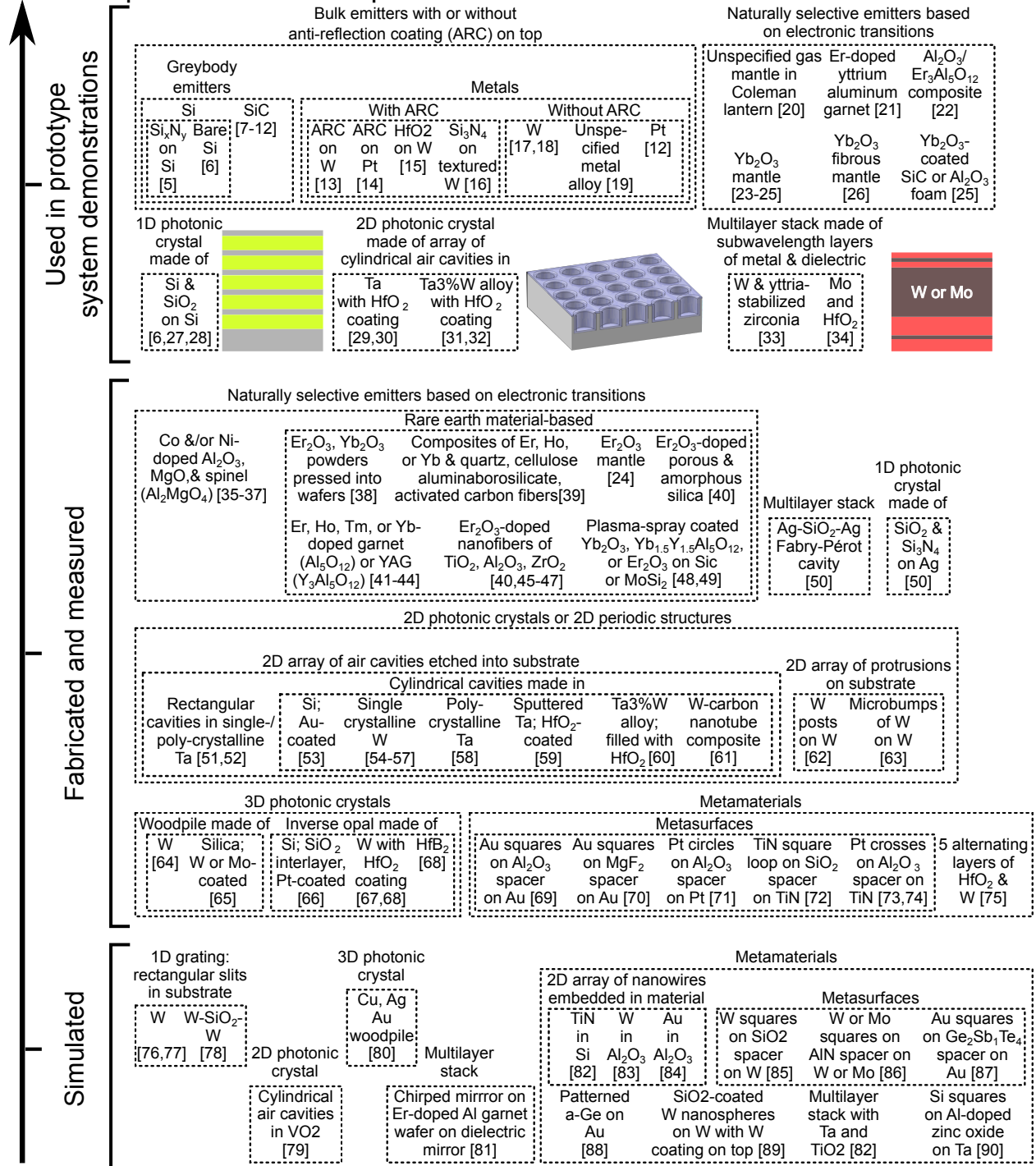


Fig 2 Three categories of TPV emitters include those that have been i) used in published system demonstrations of TPV prototypes ii) fabricated and measured and iii) simulated. The emitters in this figure emit in approximately 1-3 μm range. Abbreviations and some terminology: atomic symbols are used, ARC is an anti-reflection coating, a photonic crystal is a periodic structure,⁴ and a metamaterial is a manmade material that has optical properties not usually found in nature, metasurfaces are a class of metamaterials that consist of a 2D array of metal features on a dielectric spacer on a metal substrate.

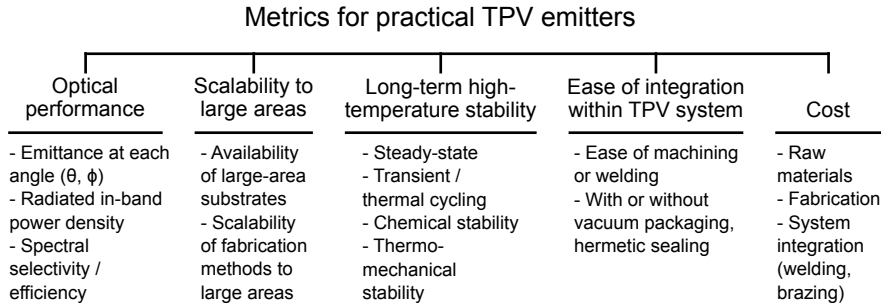


Fig 3 The proposed five metrics for practical TPV emitters include 1) optical performance 2) ability to scale to large areas 3) long-term high-temperature stability 4) ease of integration within the TPV system and 5) cost. Each has sub-metrics as shown.

slightly above the PV cell bandgap. Typically, broadband emitters yield higher output electrical power density while narrow-band emitters can increase the TPV conversion efficiency.⁹¹

The purpose of angular control, which is often an implicit aspect of spectral control, is to ensure spectral control over all angles (polar and azimuthal, θ and ϕ), because an emitter radiates photons over a wide range of angles (see Figure 4b). This is especially important because most thermal radiation is off-normal as according to Lambert’s law.

For TPV, the wavelength regions of interest are around 1-3 μm , approximately the regions of peak emission. For an emitter heated to realistic temperatures of 1000-1500 K, the peak emission wavelengths are 1.9-2.9 μm , as according to Wien’s displacement law. As such, one of the main requirements of TPV is to have low-bandgap PV cells, with typical bandgaps in the range of about 0.50-0.74 eV or 1.7-2.3 μm .

Although a PV cell can generate electricity only from in-band photons, a real emitter emits both in-band and out-of-band photons at any given angle. This leads to the following problems: a) if out-of-band photons reach the PV cell, they overheat the PV cell and reduce the PV cell efficiency and b) when out-of-band photons are emitted and not recovered, this leads to both reduced heat-to-radiation efficiency and emitter temperature.

While we have initially defined good optical performance as that achieved by designing selective

emitters, there are actually two main approaches of spectral control. The first is to enhance in-band and suppress out-of-band emission via selective emitters. The second is to reflect out-of-band photons back to the emitter, or photon recycling, via cold side filters or reflectors (CSFR) in front of (front side filter) or behind the PV cell (back surface reflector). (These are shown in Figure 1.) It is also possible to combine both approaches, for example to have a selective emitter and a filter or reflector, or even all three in theory.

Although an emitter with a CSFR performs better than a blackbody or greybody (relatively higher temperature and mitigated PV cell efficiency reduction), it suffers from view factor and absorption losses. In view factor loss, which is inherent to systems with diffuse emitters, photons are lost in the finite gap between the emitter and the filter/reflector (Figure 4c), and in absorption loss photons are absorbed at any interface (at the filter, reflector, or PV cell). Although it is possible to reduce the view factor loss by reducing the emitter area relative to the PV cell area, keeping an emitter arbitrarily small decreases its absolute radiated power.

On the other hand, selective emitters suppress out-of-band emission relative to in-band emission. This reduces view factor and absorption losses for out-of-band photons, although both losses, especially view factor losses, remain significant for in-band photons.

For the approach of selective emitters, the objective is to find or engineer a TPV emitter that emits mostly in-band photons and little to no out-of-band photons. While this is not within the scope of this review, there are many design questions regarding specific emission characteristics:

- Is it better to prioritize high in-band emission, even if the out-of-band emission is moderately high, or to prioritize low out-of-band emission, even if the in-band emission is only moderately high?
- Is it better to prioritize broadband or narrow-band emission? Narrow-band emitters are

intended to prevent thermalization⁸² in PV cells, in which the excess energy (difference between photon and bandgap energies) is absorbed and lost. However, this comes at the cost of a reduction in the radiated in-band power density. One proposed way to mitigate thermalization, then, is to use PV cells of multiple bandgaps.⁹¹

- For engineered emitters, which is better: a) select a material with naturally high emission, and suppress it in out-of-band wavelength regions, or b) select a material with naturally low emission, and enhance it in the in-band wavelength regions? Generally, suppression of naturally high emission works only for a limited wavelength range,^{27,92} ideally the emission should be suppressed for wavelengths up to about 15 μm , which accounts for >96% of the energy emitted by a blackbody at 1000 K.

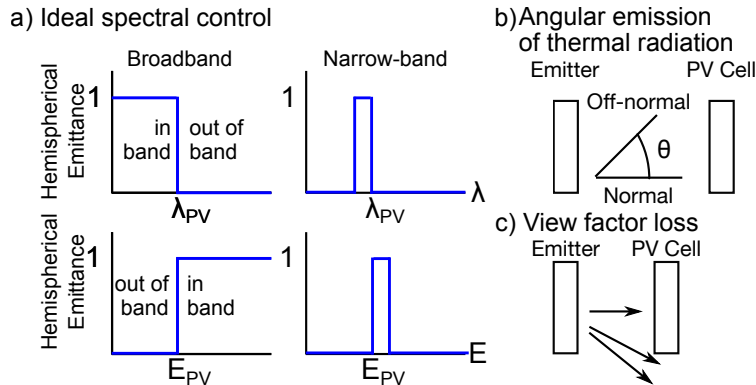


Fig 4 An emitter with good optical performance may have a) either broadband emission, where any in-band photons (energy greater or wavelength shorter than the PV cell bandgap, where E_{PV} and λ_{PV} are the bandgap energy and wavelength respectively) are preferentially emitted, or narrow-band emission, where only photons with energy slightly above the bandgap are emitted. Note that we refer to photons or radiation both in terms of energy and wavelength. b) The goal of angular control is to ensure good spectral control (preferential in-band emission) over a wide range of angles, as thermal radiation can be off-normal. c) View factor loss, where photons are lost through the emitter-PV cell gap, is a significant source of loss.

However, an emitter is not better than others simply because it has reached high temperatures, because temperatures beyond 1500 K are hard to achieve, the amount of input power required to heat an emitter may vary widely, and it is unclear if a given emitter can sustain high optical performance

at high temperature for prolonged periods. The issue of stability at high temperature is discussed as another metric later on.

One sub-metric is the in-band radiated power density $M_{\text{rad, in}}$ because the ultimate system goal is to have high output electrical power, which is enabled by maximizing the in-band power density that is emitted and can be converted.

The radiated in-band power density $M_{\text{rad, in}}$, can be calculated from the hemispherical emittance ε' , the cutoff or bandgap wavelength λ_{PV} , and the blackbody spectrum $e_b(\lambda, T)$:⁹³

$$M_{\text{rad, in}} = \pi \int_0^{\lambda_{PV}} \varepsilon'(\lambda, T) e_b(\lambda, T) d\lambda \quad (1)$$

The hemispherical emittance ε' is the emittance across all angles, where the emittance is a measure of how close the emission is to that of a blackbody. Ideally, the in-band emittance ε'_{in} is close to 1, while the out-of-band emittance $\varepsilon'_{\text{out}}$ is close to 0. In addition, the hemispherical emittance is temperature dependent, as the optical properties of a material change with temperature.

$$\varepsilon'(\lambda, T) = \frac{1}{\pi} \int_0^{2\pi} \int_0^{\pi/2} \varepsilon(\lambda, T, \theta, \phi) \cos \theta \sin \theta d\theta d\phi \quad (2)$$

However, many papers often report only the emittance at a single angle at room temperature, since it is difficult to measure the emittance across all angles as well as at high temperature.

The common metric spectral selectivity or spectral efficiency η_{sp} , which is the fraction of the radiated energy that is convertible by the PV cell, can be calculated using the hemispherical emittance:^{94,95}

$$\eta_{\text{sp}} = \frac{\int_0^{\lambda_{PV}} \varepsilon'(\lambda, T) e_b(\lambda, T) d\lambda}{\int_0^{\infty} \varepsilon'(\lambda, T) e_b(\lambda, T) d\lambda} \quad (3)$$

It is important to point out that spectral selectivity describes in-band emission relative to the total or

out-of-band emission and is distinct from the absolute values of in-band and out-of-band emittance. In other words, it is possible to have a highly selective emitter with low absolute in-band emittance or an emitter that has high in-band emittance but low selectivity (such as a greybody emitter).

Finally we are also interested in the efficiency of the radiated in-band power to the input power, $\eta_{\text{ri-input}}$, which is calculated from the radiated in-band power density $M_{\text{rad,in}}$, the area of the emitter A_{emitter} , and the input power P_{input} :

$$P_{\text{rad,in}} = M_{\text{rad,in}} A_{\text{emitter}} \quad (4)$$

$$\eta_{\text{ri-input}} = P_{\text{rad,in}} / P_{\text{input}} \quad (5)$$

One qualitative metric, which we do not use in our evaluation, is that the design of the emitter itself should be robust to fabrication imperfections across a large area, such as the lack of uniformity in critical feature dimensions. For example, a very thin film with 30 nm thickness is less robust to effects of surface roughness compared to a much thicker film.

3.2 Scalability to large areas

Because the fundamental limit for emitters is on the power radiated per unit area, one way to increase the absolute radiated power is by increasing the emitter area (its macroscopic exterior dimensions).

In terms of practical implementation, it is important to consider the following: 1) the substrates must be available in large sizes 2) the fabrication methods should accommodate large-area samples relatively easily. For example, for 1, the single-crystalline substrates of tungsten and tantalum are typically available in small diameters 1-1.5 cm (area $\sim 3 - 7 \text{ cm}^2$),^{33,57,58} while naturally selective emitters made of rare earth metals can be on the order of tens of cm^2 .²³⁻²⁵ An example for 2 is that

electron beam lithography (EBL), which is typically used for features <500 nm, is both costly and time-consuming. The overall complexity of the fabrication process, including the number of steps and the complexity of each individual step, can impact the scalability as well as the cost. However, many of the fabrication techniques used in papers may be those best suited for proof-of-concept demonstrations, rather than mass production.

3.3 Long-term high-temperature stability

The TPV emitter must sustain its optical performance at high temperatures for extended periods of time, either continuously or over multiple thermal cycles.

However, at high temperatures the kinetic energy of atoms increases and atoms diffuse more easily, leading to a number of potential thermodynamic effects:¹

- Sharp edges and features can become more rounded.^{51,67,68,96–100}
- A phase change may occur (e.g. the emitter might melt),¹⁰¹ accompanied also by changes in morphology and optical properties.⁵¹ This can happen also for crystalline phases.⁴⁵ However, it is important to keep in mind that the melting point of a material at nanometer scale is lower than for bulk.¹⁰¹
- The sizes of grains can grow in polycrystalline materials.^{51,58,96–100,102,103} However, this can actually stabilize the material, so some substrates such as polycrystalline tantalum are annealed prior to use.⁵⁸ It is also possible to use large-grain or single crystal substrates.^{51,57,102,104,105}
- Chemical degradation may occur, such as the formation of tungsten oxides^{96,97,99,100} and tantalum carbide.^{102,105} This can necessitate that the emitter operate in inert atmosphere or vacuum,^{97,99,100} which requires special packaging and complicates the TPV system integration. Chemical degradation of 2D and 3D tungsten and 2D tantalum photonic crystals can be

mitigated by capping the surface with a 20 - 40 nm protective coating of hafnium dioxide (HfO_2).^{1,67,68,102-104} One comparison of HfO_2 and Al_2O_3 in 3D photonic crystals⁶⁷ has found HfO_2 to be more thermally robust than Al_2O_3 , but Al_2O_3 is less expensive and has been used to protect a metasurface emitter.⁷³

- Thermal expansion could lead to the cracking of a material.^{67,68,95,103} Also emitters with interfaces between different materials are at risk of delamination because different materials have different thermal expansion coefficients.

Some strategies for improving the high-temperature stability include selecting materials that are known to have good high temperature properties, alloying to promote a solute drag effect,^{97,99,100} and modifying the geometry of a structure to change diffusion rates.^{100,106}

There do not appear to be any published long-term (>1000 hours) studies; in some cases it appears the emitter is only heated to measure its high-temperature optical properties. One long study is 168 hours (7 days) at 1000 °C (1273 K) for a 2D structure made with tungsten and carbon nanotubes.⁶¹ We have included some studies of emitter stability at high temperatures in Table 1.

The longest reported studies we know of are 300 hours each for an erbium-doped yttrium aluminum garnet (Er-YAG) crystal used in a solar TPV system²¹ and a 2D photonic crystal made of tantalum-tungsten alloy and capped with 20-40 nm HfO_2 ¹ used in a radioisotope TPV prototype.³¹ The former cracked and darkened after 300 hours in the sun, although the authors attribute it potentially to a water leak. The 2D photonic crystal showed little to no degradation in optical performance after annealing for 300 hours at 1000 °C (1273 K)¹ and also 1 hour at 1200 °C (1473 K).¹⁰⁴

The only other emitters we know of that were used in both system demonstrations and some high-temperature stability experiments include a Yb_2O_3 foam ceramic,²⁵ a 2D photonic crystal

made of polycrystalline tantalum and coated with 20-40 nm HfO₂,¹⁰² and a multilayer stack made of tungsten and HfO₂.³⁴ The foam ceramic was robust under 200 thermal cycles, the 2D tantalum photonic crystal showed no visible degradation after 144 hours at 900 °C (1173 K) and 1 hour at 1000 °C (1273 K),¹⁰² and the multilayer stack showed little to no degradation after at least 1 hour at 1423 K in vacuum $<5 \times 10^{-2}$ Pa and two rapid thermal cycles up to 1250 K, but showed degradation after 1 hour at 1473 K.

3.4 Ease of integration within the TPV system

The design choices for the emitter can present several challenges for its integration within the TPV system, in particular when 1) putting the emitter and heat source physically together for thermal contact and 2) packaging the system for operation in vacuum or inert gas environment.

In some cases the emitter and heat source are made out of the same material such as silicon carbide¹² or platinum,¹² or the emitter is directly fabricated onto the heat source, for example through the deposition of emitter materials silicon and silicon dioxide^{6,27} or tantalum⁵⁹ onto a microcombustor, or the fabrication of a combined absorber/emitter for solar TPV.^{16,33,34}

In other cases it may be required to cut the emitter to the correct size and to machine and weld it onto the heat source, such as a microcombustor. It is possible to use foil, sputtered coating, or a solid state substrate. In the last case especially, the mechanical properties of the emitter material becomes significant. As an example, three different substrates have been explored in the development of 2D photonic crystal emitters. These include single crystalline tungsten, polycrystalline tantalum and tantalum-tungsten alloy.^{57,58,104} Tungsten is brittle and difficult to machine and weld,⁵⁸ while polycrystalline tantalum is more compliant and easier to weld and machine but is soft so needs to be thicker than tungsten to achieve the same mechanical stability. Tantalum-tungsten alloy

Emitter	Used in system demo.?	Length	Temp. (K)	Environment	Result
Al ₂ O ₃ -coated W 3D inverse opal photonic crystal ⁶⁷	-	12 h	1273	Forming gas, 5% H ₂ in Ar	Little to no degradation
Same as above	-	12 h	1673	Forming gas, 5% H ₂ in Ar	Collapse of structure
HfO ₂ -coated W 3D inverse opal photonic crystal ⁶⁷	-	12 h	1273	Forming gas, 5% H ₂ in Ar	Little to no degradation
Same as above	-	12 h	1673	Forming gas, 5% H ₂ in Ar	Some grain growth, increased surface roughness
W-coated 3D inverse opal photonic crystal ⁶⁸	-	12h	1273	-	Little to no degradation
Same as above	-	-	>1273	-	Collapse of structure
W inverse 3D inverse opal photonic crystal ⁶⁸	-	12h	1273	-	Little to no degradation
20 nm-HfO ₂ -coated W inverse 3D inverse opal photonic crystal ⁶⁸	-	1h	1673	-	Little to no degradation
2D structure made with W, carbon nanotubes ⁶¹	-	168h, 7 days	1273	1 × 10 ⁻³ Torr with He protection	Little to no degradation
Single crystal Er doped yttrium aluminum garnet ²¹	Yes	300h	In sun	In sun	Emitter cracked and darkened, but may be due to water leak
2D photonic crystal made of Ta3%W alloy w/ HfO ₂ coating ¹	Yes ^{31,32}	300h	1273	Vacuum (5 × 10 ⁻⁶ Torr)	Little to no degradation
Same as above ¹⁰⁴	Yes ^{31,32}	1h	1473	Vacuum (5 × 10 ⁻⁶ Torr)	Little to no degradation
Yb ₂ O ₃ foam ceramic ²⁵	Yes	200 cycles	-	-	Little to no degradation
2D photonic crystal made of polycrystalline Ta w/ HfO ₂ coating ¹⁰²	Yes ^{29,30}	144h, 6 days	1173	Ar, ~100 mTorr	Little to no degradation
Same as above	Yes ^{29,30}	1h	1273	Ar, ~100 mTorr	Little to no degradation
A multilayer stack made of W and HfO ₂ ¹⁰⁷	Yes ³⁴	>1h	1473	Vacuum, <5 × 10 ⁻² Pa	Degradation
Same as above	Yes ³⁴	2 rapid thermal cycles	1250 max	-	Little to no degradation

Table 1 A few (this list is not exhaustive) studies of high-temperature stability of TPV emitters.

combines the better thermomechanical properties of tungsten with tantalum's ability to be more easily machined and welded.^{1,104}

In addition, high temperature stability concerns also apply: operating the heat source and emitter and high temperatures can lead to cracking and delamination of the emitter or heat source.

Also, the emitter often must be in vacuum or inert gas environment in order to prevent chemical degradation processes such as oxidation and heat losses due to convective heat transfer processes.

In our comparison of system demonstrations of prototype TPV, we have noted where the system was operated under vacuum or inert atmosphere, and whether the emitter was fabricated onto or together with the heat source.

3.5 *Cost*

The overall cost of emitter production depends on the cost of the raw materials, fabrication, as well as system integration. In particular, many emitters make use of relatively scarce materials such as hafnium and rare earth metals. The cost of fabrication may increase with increased number of processing steps or complexity of fabrication processes.

For our evaluation, because it is generally difficult to project the cost, considering the emitter area can be scaled and improvements in fabrication technology may reduce costs, we have not done any assessment.

4 At-a-glance evaluation of emitters used in prototype system demonstrations

In Table 2 we summarize reported features of the emitters that have been implemented in prototype system demonstrations. In this table we show the cutoff wavelength (which corresponds to the bandgap of the PV cell used in the system demonstration), the average in-band emittance ϵ_{in} , the

average out-of-band emittance ε_{out} , the emittance measurement angle θ , the emitter temperature T_{emitter} , whether we have found high temperature studies, whether the system is operated in vacuum or an inert gas environment, and whether the emitter is fabricated onto or with the heat source.

The Appendix (Section A) contains tables with more details, including estimations of the in-band radiated power density (power per area) $M_{\text{rad,in}}$ and the absolute in-band radiated power to input power efficiency, $\eta_{\text{ri-input}}$. Because spectral selectivity η_{sp} is a commonly reported metric, and also in part because many papers do not report the long-wavelength emittance, we have not included this in our evaluation.

Broadly there are five types of emitters that have been implemented in prototype system demonstrations (the emitters in Table 2 are organized by these types, in this order):

1. Bulk emitters

(a) Greybody emitters such as silicon and silicon carbide⁵⁻¹² are typically inexpensive, easy to fabricate in large areas, and often can be fabricated onto or with the heat source. However, they have both high in-band emission and out-of-band emission, which is why they are often coupled with cold side filters.

(b) Metals with¹³⁻¹⁶ or without ARC^{12,17-19} can be easy and inexpensive to fabricate in large areas. The emission depends on the metal optical properties; the role of the ARC layer is typically to enhance emittance in a narrow band around the bandgap.

2. Naturally selective emitters^{20-26,108,109} have been made primarily from rare earth metals, especially erbium and ytterbium. They are easy to fabricate in large areas and with high-temperature stability, especially by doping high-temperature ceramics. However the emission wavelength range of naturally selective emitters is not tunable and narrow-band, which can lead to low in-band emitted power density.

3. 1D photonic crystals,^{6,27,28} also known as dielectric mirrors, consist of alternating layers of materials with a high contrast in indices of refraction. Interference effects in this structure lead to a fairly broad reflection bandwidth, which can be used to suppress high natural emittance of a material for a wavelength region. They are easy and inexpensive to fabricate at large areas, but have multiple interfaces and are not typically made from high-temperature materials though can be directly fabricated onto a heat source. They may have high out-of-band emission outside of the region of suppression.
4. 2D photonic crystals²⁹⁻³² for TPV typically are a 2D array of features on top of or in a substrate, such as cylindrical posts or air cavities, with feature sizes on the order of the wavelength of interest. For photonic crystals with air cavities, each individual cavity acts as a waveguide to enhance emission of wavelengths below a cutoff (half a wavelength corresponds roughly to the cavity diameter). Whether an emitter can be fabricated inexpensively with large area and can be integrated with the heat source depends largely on the substrate, for which a high-temperature material is often used.
5. The multilayer stacks^{33,34} (which differ from 1D photonic crystals in that there is no periodicity in the thicknesses of the layers) featured in this review are combined absorber/emitters for solar TPV, that consist of alternating metal and dielectric layers of varying thicknesses. The layer thicknesses, which are sometimes subwavelength, are optimized to enable both broadband absorption and emission. Although the optical performance is good and the fabrication costs likely low, the ability to fabricate large areas depends on the available sizes of the metal. Although high temperature materials are used, there are many interfaces and the long-term high-temperature stability is unclear.

Emitter	Cutoff (μm)	ϵ_{in}	ϵ_{out}	θ	T_{emitter} (K)	Area (cm^2)	High temp. studies?	Vacuum/inert?	Emitter fab. w/ heat src?
Si ⁶	2.27	-	-	-	1013	1	-	Yes	Yes
Si _x N _y -coated Si ⁵	1.72	0.7	0.7	all	1043	-	-	-	Yes
SiC, with filter ⁷	1.8	-	-	-	-	101.4	-	-	-
SiC, with filter ⁸	1.7	0.5	0.5	45°	1053	-	-	-	-
Commercial SiC burner ^{9,10}	1.8	-	-	-	1323	-	-	-	Yes
SiC, with filter ¹¹	2.07	-	-	-	1312	29.16	-	-	-
Combined emitter-combustor: SiC ¹²	1.8	-	-	-	1120	-	-	-	Yes
ARC on W on SiC ¹³	1.8	0.86	0.27	-	1548	469	-	-	-
ARC-coated Pt foil ¹⁴	1.8	-	-	-	1287	>38	-	Yes	-
HfO ₂ -coated W foil ¹⁵	1.88	-	-	-	1300-1500	2.83	-	Yes	-
Absorber/emitter: Si ₃ N ₄ -coated, textured W ¹⁶	1.8	0.611	0.052	-	1456	6.25	-	Yes	Yes
W-coated SiSiC ¹⁷	1.8	-	-	-	1463	118.8	-	Yes	Yes
Combined emitter-combustor: Pt ¹²	1.8	0.099	0.044	-	1450	-	-	-	Yes
Burner made of unspecified "super alloy" ¹⁹	1.73	-	-	-	1458	1282	-	-	Yes
Absorber/Emitter: W (Ta?) foil ¹⁸	1.82	0.69	0.42	-	1720	1.67	-	-	-
Same as above, larger area ¹⁸	1.82	0.74	0.52	-	1400	5.09	-	-	-
Commercial gas mantle ^{20,108}	1.1	-	-	-	1570-1970	-	-	-	-
Absorber/emitter: SiC plate, Emitter: Er-YAG ²¹	1.1, 1.65	-	-	-	1133-1473	-	Yes ²¹	-	-
Al ₂ O ₃ /Er ₃ Al ₅ O ₁₂ composite, with pinhole ²²	1.8	0.41	0.25	-	1254	1	-	-	-
Yb ₂ O ₃ mantle, with filter ²³	1.1	-	-	-	-	231.7	-	-	-
Yb ₂ O ₃ fibrous mantle ²⁶	1.1	-	-	-	-	-	-	-	-
Yb ₂ O ₃ mantle ^{24,25}	1.1	0.63	-	-	1735	75	-	-	-
Yb ₂ O ₃ -coated Al ₂ O ₃ or SiC foam ceramic ^{25,109}	1.1	-	-	-	~1735?	-	Yes ²⁵	-	-
1D PhC of Si, SiO ₂ on Si microreactor ⁶	2.27	-	-	-	1073	1	-	Yes	Yes
1D PhC of Si, SiO ₂ on Si ²⁷	2.25	0.86	0.32	-	1285	1	-	Yes	Yes
1D PhC of Si, SiO ₂ , on Si with filter ²⁸	2.25	-	-	-	-	4	-	Yes	Yes
HfO ₂ -coated, 2D PhC made in polycrystalline Ta ²⁹	2.3	0.52	0.29	all	1270	-	Yes ¹⁰²	Yes	Yes
HfO ₂ -coated, 2D PhC made in polycrystalline Ta ³⁰	2.0	0.58	0.18	all	1327	4.41	Yes ³⁰	Yes	No
HfO ₂ -coated, 2D PhC made in Ta3%W alloy ^{31,32}	2.25	0.75	0.26	-	1233	1	Yes ^{1,104}	Yes	No
Combined emitter-absorber: W, yttria-stabilized zirconia multilayer stack ³³	1.85	0.84	0.21	-	1640	1.77	-	Yes	Yes
Combined emitter-absorber: Mo, HfO ₂ multilayer stack ³⁴	1.85	0.71	0.15	all	1640	0.636	Yes ¹⁰⁷	Yes	Yes

Table 2 At-a-glance summary of prototype TPV system demonstrations. PhC = photonic crystal.

5 Conclusion

In our review we have presented five metrics for evaluating the practicality of TPV emitters and have used this approach to evaluate the five broad categories of emitters that have been used in TPV system prototypes. We have categorized emitters in the literature based on whether they have been used in prototype system demonstrations, fabricated, or simulated, and have evaluated the emitters in the first category according to our metrics. The emitters in this category include bulk emitters, naturally selective emitters, 1D photonic crystals, 2D photonic crystals, and multilayer stacks. The metrics for a practical TPV emitter include optical performance, scalability to large areas, long-term high temperature stability, ease of integration within a TPV system, and cost.

However, none of the emitters or types of emitters identified have yet satisfied all five criteria for practical TPV emitters. An emitter with good optical performance shows high, broadband, preferential in-band emittance. Some emitters with promising optical performance include the 1D photonic crystal, 2D photonic crystal, and multilayer stacks. For the latter two types, there have been some studies on the high-temperature stability and system integration. The multilayer stack is fabricated directly with the absorber (heat source), but its high-temperature stability has not been shown beyond one hour. On the other hand, a 2D photonic crystal made in refractory metals that can be fabricated on the order of cm^2 has some slightly high out-of-band emittance but has been successfully integrated with microcombustor heat sources and has shown promising high-temperature stability of a few hundred hours at 900-1000 °C.

Moving forward, studies on the practical aspects of each TPV emitter, such as the five metrics we have presented in this review, are critical for the maturation of TPV technology. We have yet to find an emitter that satisfies the following performance metrics: spectral selectivity exceeding 90-95%,

high in-band emittance of 0.9-0.95, and high-temperature stability on the order of thousands of hours and hundreds of cycles (a typical Li ion battery lasts 2-3 years and ~ 500 cycles¹¹⁰). Both of these as well as large-area fabrication can be addressed independently of the overall TPV system setup. One promising new class of emitter is metamaterials, which show high optical performance; however, studies of high-temperature stability are at the moment limited. The ability of TPV systems to be commercialized hinges on the practical attributes of selective emitters, for which our five-metric approach can serve as a framework.

Acknowledgments

This work was supported by the Army Research Office through the Institute for Soldier Nanotechnologies under Contract No. W911NF-13-D-0001, the Micro Autonomous Systems and Technology Collaborative Technology Alliance under Contract No. 892730, the Solid-State Solar-Thermal Energy Conversion Center (S3TEC), an Energy Frontier Research Center funded by the U.S. Department of Energy (DOE), Office of Science, Basic Energy Sciences (BES), under Award No. DE-SC0001299/ DE-FG02-09ER46577. R.S. would like to acknowledge Samantha Dale Strasser of the MIT EECS Communication Lab for help with the manuscript.

References

- 1 V. Stelmakh, *A Practical High Temperature Photonic Crystal for High Temperature Thermophotovoltaics*. PhD thesis, Massachusetts Institute of Technology (2017).
- 2 V. Rinnerbauer, S. Ndao, Y. Yeng, *et al.*, “Recent developments in high-temperature photonic crystals for energy conversion,” *Energy Environ. Sci.* **5**, 8815–8823 (2012).

- 3 N. Pfister and T. Vandervelde, “Selective emitters for thermophotovoltaic applications,” *Phys. Status. Solidi A* **214**(1) (2017).
- 4 J. Joannopoulos, S. Johnson, J. Winn, *et al.*, *Photonic Crystals*, Princeton University Press, second ed. (2008).
- 5 O. Nielsen, L. Arana, C. Baertsch, *et al.*, “Thermophotovoltaic micro-generator for portable power applications,” in *Transducers, Solid-State Sensors, Actuators and Microsystems, 12th International Conference on*, **1**, 714–717 (2003).
- 6 W. Chan, P. Bermel, R. Pilawa-Podgurski, *et al.*, “Toward high-energy-density, high-efficiency, and moderate-temperature chip-scale thermophotovoltaics,” *Proc. Natl. Acad. Sci. U.S.A.* **110**(14), 5309–5314 (2013).
- 7 L. Fraas, “Small efficient thermophotovoltaic power supply using infrared-sensitive gallium antimonide cells,” Tech. Rep. DAAG55-97-C-0002, U.S. Army Research Office (1996).
- 8 E. Horne, “Hybrid thermophotovoltaic power systems,” tech. rep., EDTEK, Inc. (2002).
- 9 C. Astle, G. Kovacik, and T. Heidrick, “Design and preliminary testing of a prototype thermophotovoltaic system,” *Proceedings of IMECE* (2003).
- 10 C. Astle, G. Kovacik, and T. Heidrick, “Design and performance of a prototype thermophotovoltaic system,” *Journal of Solar Energy Engineering* **129**, 340–342 (2007).
- 11 B. Wernsman, R. Siemiej, S. Link, *et al.*, “Greater than 20% radiant heat conversion efficiency of a thermophotovoltaic radiator/module system using reflective spectral control,” *IEEE Transactions on Electron Devices* **51**(3), 512–515 (2004).
- 12 W. Yang, S. Chou, C. Shu, *et al.*, “Research on micro-thermophotovoltaic power generators with different emitting materials,” *J. Micromech. Microeng.* **15**, S239 (2005).

- 13 L. Fraas, J. Samaras, J. Avery, *et al.*, “Antireflection coated refractory metal matched emitters for use with GaSb thermophotovoltaic generators,” *IEEE* (2000).
- 14 E. Doyle, K. Shukla, and C. Metcalfe, “Development and demonstration of a 25 watt thermophotovoltaic power source for a hybrid power system,” Tech. Rep. TR04-2001, National Aeronautics and Space Administration (2001).
- 15 A. Datas and C. Algora, “Development and experimental evaluation of a complete solar thermophotovoltaic system,” *Prog. Photovol. Res. Appl.* **21**, 1025–1039 (2013).
- 16 C. Ungaro, S. Gray, and M. Gupta, “Solar thermophotovoltaic system using nanostructures,” *Optics Express* **23**(19) (2015).
- 17 T. Aicher, P. Kästner, A. Gopinath, *et al.*, “Development of a novel TPV power generator,” *AIP Conference Proceedings* **738**, 71 (2004).
- 18 V. Andreev, A. Vlasov, V. Khvostikov, *et al.*, “Solar thermophotovoltaic converters based on tungsten emitters,” *Journal of Solar Energy Engineering* **129**, 298–303 (2007).
- 19 K. Qiu, A. Hayden, and E. Entchev, “TPV power generation system using a high temperature metal radiant burner,” *AIP Conference Proceedings* **890**, 27–36 (2007).
- 20 H. Kolm, “Solar-battery power source,” Quarterly Progress Report, Solid State Research, Group 35 35, MIT Lincoln Laboratory (1956).
- 21 K. Stone, D. Chubb, D. Wilt, *et al.*, “Testing and modeling of a solar thermophotovoltaic power system,” *AIP Conference Proceedings* **199**, 199–209 (1996).
- 22 H. Yugami, H. Sai, K. Nakamura, *et al.*, “Solar thermophotovoltaic using Al₂O₃/Er₃Al₅O₁₂ eutectic composite selective emitter,” *IEEE Photovoltaic Spec. Conf.* **28**, 1214–1217 (2000).

- 23 K. Chen, D. Osborn, P. Sarmiento, *et al.*, “Small, efficient thermophotovoltaic power supply,” Tech. Rep. DAAG55-97-C-0003, U.S. Army Research Office (1999).
- 24 B. Bitnar, W. Durisch, J.-C. Mayor, *et al.*, “Characterisation of rare earth selective emitters for thermophotovoltaic applications,” *Solar Energy Materials and Solar Cells* **73**, 221–234 (2002).
- 25 S. Bitnar, W. Durisch, G. Palfinger, *et al.*, “Practical thermophotovoltaic generators,” *Semiconductors* **28**, 941–945 (2004).
- 26 R. Nelson, “TPV systems and state-of-art development,” in *Fifth Conference on Thermophotovoltaic Generation of Electricity*, T. J. Coutts, G. Guazzoni, and J. Luther, Eds., *American Institute of Physics Conference Series* **653**, 3–17 (2003).
- 27 A. Lenert, D. Bierman, Y. Nam, *et al.*, “A nanophotonic solar thermophotovoltaic device,” *Nature Nanotechnology* **9**, 126–130 (2014).
- 28 D. Bierman, A. Lenert, W. Chan, *et al.*, “Enhanced photovoltaic energy conversion using thermally based spectral shaping,” *Nature Energy* **1** (2016).
- 29 V. Rinnerbauer, A. Lenert, D. Bierman, *et al.*, “Metallic photonic crystal absorber-emitter for efficient spectral control in high-temperature solar thermophotovoltaics,” *Adv. Energy. Mater.* (2014).
- 30 W. Chan, V. Stelmakh, M. Ghebrebrhan, *et al.*, “Enabling efficient heat-to-electricity generation at the mesoscale,” *Energy Environ. Sci.* **10**, 1367 (2017).
- 31 X. Wang, W. Chan, V. Stelmakh, *et al.*, “Prototype of radioisotope thermophotovoltaic system using photonic crystal spectral control,” *J. Phys.: Conf. Ser.* **660**, 012034 (2015).

- 32 X. Wang, *Toward high efficiency radioisotope thermophotovoltaic system by spectral control*. PhD thesis, Massachusetts Institute of Technology (2017).
- 33 M. Shimizu, A. Kohiyama, and J. Yugami, “High-efficiency solar-thermophotovoltaic system equipped with a monolithic planar selective absorber/emitter,” *J. Photon. Energy* **5**, 053099 (2015).
- 34 A. Kohiyama, M. Shimizu, and H. Yugami, “Unidirectional radiative heat transfer with a spectrally selective planar absorber/emitter for high-efficiency solar thermophotovoltaic systems,” *Appl. Phys. Express* **9**, 112302 (2016).
- 35 L. Ferguson and L. Fraas, “Matched infrared emitters for use with GaSb TPV cells,” *AIP Conference Proceedings* **401**, 169–179 (1997).
- 36 L. Ferguson and F. Dogan, “A highly efficient NiO-doped MgO matched emitter for thermophotovoltaic energy conversion,” *Mater. Sci. Eng. B* **83**, 35–41 (2001).
- 37 L. Ferguson and F. Dogan, “Spectral analysis of transition metal-doped MgO ‘matched emitters’ for thermophotovoltaic energy conversion,” *J. Mater. Sci.* **37**, 1301–1308 (2002).
- 38 G. Guazzoni, “High-temperature spectral emittance of oxides of erbium, samarium, neodymium and ytterbium,” *Applied Spectroscopy* **26**(1), 60–65 (1972).
- 39 P. Adair and M. Rose, “Composite emitters for TPV systems,” *AIP Conference Proceedings* **321**, 245 (1995).
- 40 A. Licciulli, A. Maffezzoli, D. Diso, *et al.*, “Sol-gel preparation of selective emitters for thermophotovoltaic conversion,” *Journal of Sol-Gel Science and Technology* **26**, 1119–1123 (2003).

- 41 D. Chubb, A. Pal, M. Patton, *et al.*, “Rare earth doped high temperature ceramic selective emitters,” *Journal of the European Ceramic Society* **19**, 2551–2562 (1999).
- 42 M. G. Krishna, M. Rajendra, D. Pyke, *et al.*, “Spectral emissivity of ytterbium oxide-based materials for application as selective emitters in thermophotovoltaic devices,” *Sol. Energy Mater. Sol. Cells* **59**, 337–348 (1999).
- 43 A. Licciulli, A. Maffezzoli, D. Diso, *et al.*, “Porous garnet coatings tailoring the emissivity of thermostructural materials,” *J. Sol-Gel Sci. Technol.* **32**, 247–251 (2004).
- 44 R. A. Lowe, D. L. Chubb, S. C. Farmer, *et al.*, “Rare-earth garnet selective emitter,” *Appl. Phys. Lett.* **64**, 3551 (1998).
- 45 V. Tomer, R. Teye-Mensah, J. Tokash, *et al.*, “Selective emitters for thermophotovoltaics: erbia-modified electrosopun titania nanofibers,” *Solar Energy Materials and Solar Cells* **85**, 477–488 (2005).
- 46 R. Teye-Mensah, V. Tomer, W. Kataphinan, *et al.*, “Erbia-modified electrospun titania nanofibres for selective infrared emitters,” *J. Phys.: Condens. Matter.* **16**, 7555–7564 (2004).
- 47 D. Diso, A. Licciulli, A. Bianco, *et al.*, “Erbium containing ceramic emitters for thermophotovoltaic energy conversion,” *Mater. Sci. Eng. B* **B98**, 144–149 (2003).
- 48 H. Wang, H. Ye, and Y. Zhang, “Preparation and performance evaluation of Er₂O₃ coating-type selective emitter,” *Sci. China Technol. Sci.* **57**, 332–338 (2014).
- 49 W. Tobler and W. Durisch, “Plasma-spray coated rare-earth oxides on molybdenum disilicide – high temperature stable emitters for thermophotovoltaics,” *Applied Energy* **85**, 371–383 (2008).

- 50 B. Lee and Z. Zhang, “Design and fabrication of planar multilayer structures with coherent thermal emission characteristics,” *J. Appl. Phys.* **100**, 1–10 (2007).
- 51 H. Sai, Y. Kanamori, and H. Yugami, “High-temperature resistive surface grating for spectral control of thermal radiation,” *Appl. Phys. Lett.* **82**(11), 1685–1687 (2003).
- 52 H. Sai and H. Yugami, “Thermophotovoltaic generation with selective radiators based on tungsten surface gratings,” *Appl. Phys. Lett.* **85**, 3399 (2004).
- 53 M. U. Pralle, N. Moelders, M. P. McNeal, *et al.*, “Photonic crystal enhanced narrow-band infrared emitters,” *Appl. Phys. Lett.* **81**, 4685–4687 (2002).
- 54 N. Jovanić, I. Čelanović, and J. Kassakian, “Two-dimensional tungsten photonic crystals as thermophotovoltaic selective emitters,” *AIP Conference Proceedings* **890**, 47–55 (2008).
- 55 M. Araghchini, Y. Yeng, N. Jovanić, *et al.*, “Fabrication of two-dimensional tungsten photonic crystals for high-temperature applications,” *J. Vac. Sci. Technol. B* **29**, 61402 (2011).
- 56 I. Čelanović, N. Jovanić, and J. Kassakian, “Two-dimensional tungsten photonic crystals as selective thermal emitters,” *Appl. Phys. Lett.* **92**, 193101 (2008).
- 57 Y. Yeng, M. Ghebrebrhan, P. Bermel, *et al.*, “Enabling high-temperature nanophotonics for energy applications,” *Proc. Natl. Acad. Sci. U.S.A.* **109**(7), 2280–2285 (2012).
- 58 V. Rinnerbauer, S. Ndao, Y. Yeng, *et al.*, “Large-area fabrication of high aspect ratio tantalum photonic crystals for high-temperature selective emitters,” *J. Vac. Sci. Technol. B* **31**(1), 011802 (2013).
- 59 V. Stelmakh, W. Chan, M. Ghebrebrhan, *et al.*, “Sputtered tantalum photonic crystal coatings for high-temperature energy conversion applications,” in *IEEE Transactions on Nanotechnology*, **15**(2), 303–309 (2016).

- 60 V. Stelmakh, W. Chan, M. Ghebrebrhan, *et al.*, “Fabrication of an omnidirectional 2D photonic crystal emitter for thermophotovoltaics,” *J. Phys.: Conf. Series* **773**, 012037 (2016).
- 61 K. Cui, P. Lemaire, H. Zhao, *et al.*, “Tungsten-carbon nanotube composite photonic crystals as thermally stable spectral-selective absorbers and emitters for thermophotovoltaics,” *Adv. Energy Mater.*, 1801471 (2018).
- 62 A. Heinzl, V. Boerner, A. Gombert, *et al.*, “Radiation filters and emitters for the NIR based on periodically structured metal surfaces,” *Journal of Modern Optics* **47**(13), 2399–2419 (2000).
- 63 H. Qiao, J. Yang, F. Wang, *et al.*, “Femtosecond laser direct writing of large-area two-dimensional metallic photonic crystal structures on tungsten surfaces,” *Opt. Express* **23**(20), 26617–26627 (2015).
- 64 S. Lin, J. Moreno, and J. Fleming, “Three-dimensional photonic-crystal emitter for thermal photovoltaic power generation,” *Appl. Phys. Lett.* **93**(2), 380 (2003).
- 65 P. Nagpal, S. Hon, A. Stein, *et al.*, “Efficient low-temperature thermophotovoltaic emitters from metallic photonic crystals,” *Nano Lett.* **8**(10) (2008).
- 66 M. Garin, D. Hernández, T. Trifonov, *et al.*, “Three-dimensional metallo-dielectric selective thermal emitters with high-temperature stability for thermophotovoltaic applications,” *Sol. Energy Mater. Sol. Cells* **134**, 22–28 (2015).
- 67 K. Arpin, M. Losego, and P. Braun, “Electrodeposited 3D tungsten photonic crystals with enhanced thermal stability,” *Chem. Mater.* **23**, 4783–4788 (2011).
- 68 K. Arpin, M. Losego, A. Cloud, *et al.*, “Three-dimensional self-assembled photonic crystals with high temperature stability for thermal emission modification,” *Nat. Commun.* **4** (2013).

- 69 J. Hao, J. Wang, X. Liu, *et al.*, “High performance optical absorber based on a plasmonic metamaterial,” *Appl. Phys. Lett.* **96**, 351104 (2010).
- 70 B. Zhang, J. Hendrickson, and J. Guo, “Multispectral near-perfect metamaterial absorbers using spatially multiplexed plasmon resonance metal square structures,” *J. Opt. Soc. Am. B* **30**, 656 (2013).
- 71 C. Shemelya, D. DeMeo, N. P. Latham, *et al.*, “Stable high temperature metamaterial emitters for thermophotovoltaic applications,” *Appl. Phys. Lett.* **104**, 201113 (2014).
- 72 W. Li, U. Guler, N. Kinsey, *et al.*, “Refractory plasmonics with titanium nitride: Broadband metamaterial absorber,” *Adv. Mater.* **26**, 7959–7965 (2014).
- 73 D. Woolf, J. Hensley, J. Cederberg, *et al.*, “Heterogeneous metasurface for high temperature selective emission,” *Appl. Phys. Lett.* **105**, 0181110 (2014).
- 74 D. Woolf, E. Kadlec, D. Bethke, *et al.*, “High-efficiency thermophotovoltaic energy conversion enabled by a metamaterial selective emitter,” *Optica* **5**(2), 213–218 (2018).
- 75 P. Dyachenko, S. Molesky, A. Y. Petrov, *et al.*, “Controlling thermal emission with refractory epsilon-near-zero metamaterials via topological transitions,” *Nat. Commun.* **7**, 11809 (2016).
- 76 N. Nguyen-Huu, Y.-B. Chen, and Y.-L. Lo, “Development of a polarization-insensitive thermophotovoltaic emitter with a binary grating,” *Opt. Express* **20**(6), 5882–5890 (2012).
- 77 Y.-B. Chen and Z. Zhang, “Design of tungsten complex gratings for thermophotovoltaic radiators,” *Optics Communications* **269**, 411–417 (2007).
- 78 J. Song, H. Wu, Q. Cheng, *et al.*, “1D trilayer films grating with W/SiO₂/W structure as a wavelength-selective emitter for thermophotovoltaic applications,” *J. Quantum Spectrosc. Radiat. Transf.* **158**, 136–144 (2015).

- 79 H. Ye, H. Wang, and Q. J. Cai, “Two-dimensional VO₂ photonic crystal selective emitter,” *Quantum Spectrosc. Radiat. Transf.* **158**, 119–126 (2015).
- 80 G. B. Farfan, M. F. Su, M. M. R. Taha, *et al.*, “High-efficiency photonic crystal narrowband thermal emitters,” in *Proc. SPIE Photonic and Phononic Crystal Materials and Devices X*, A. Adibi, S.-Y. Lin, and A. Scherer, Eds., *Proc. SPIE* **7609**(76090V) (2010).
- 81 E. Sakr, Z. Zhou, and P. Bermel, “High efficiency rare-earth emitter for thermophotovoltaic applications,” *Appl. Phys. Lett.* **105**, 111107 (2014).
- 82 S. Molesky, C. Dewalt, and Z. Jacob, “High temperature epsilon-near-zero and epsilon-near-pole metamaterial emitters for thermophotovoltaics,” *Opt. Express* **21**(S1), A96–A110 (2013).
- 83 J.-Y. Chang, Y. Yang, and L. Wang, “Tungsten nanowire based hyperbolic metamaterial emitters for near-field thermophotovoltaic applications,” *Int. J. Heat Mass Transf.* **87**, 237–247 (2015).
- 84 H. Deng, T. Wang, J. Gao, *et al.*, “Metamaterial thermal emitters based on nanowire cavities for high-efficiency thermophotovoltaics,” *J. Opt.* **16**(3), 035102 (2014).
- 85 B. Zhao, L. Wang, Y. Shuai, *et al.*, “Thermophotovoltaic emitters based on a two-dimensional grating/thin-film nanostructure,” *Int. J. Heat Mass Transf.* **67**, 637–645 (2013).
- 86 C. Wu, B. N. III, J. John, *et al.*, “Metamaterial-based integrated plasmonic absorber/emitter for solar thermo-photovoltaic systems,” *J. Opt.* **14**(24005) (2012).
- 87 T. Cao, L. Zhang, R. E. Simpson, *et al.*, “Mid-infrared tunable polarization-independent perfect absorber using a phase-change metamaterial,” *J. Opt. Soc. Am.* **B30**, 1580–1585 (2013).

- 88 J. Bossard and D. Werner, “Metamaterials with angle selective emissivity in the near-infrared,” *Opt. Express* **21**(5), 5215–5225 (2013).
- 89 L. Mo, L. Yang, E. H. Lee, *et al.*, “High-efficiency plasmonic metamaterial selective emitter based on an optimized spherical core-shell nanostructure for planar solar thermophotovoltaics,” *Plasmonics* **10**, 529–538 (2015).
- 90 E. Sakr and P. Bermel, “Thermophotovoltaics with spectral and angular selective doped-oxide thermal emitters,” *Opt. Express* **25**(20) (2017).
- 91 A. Datas and A. Martí, “Thermophotovoltaic energy in space applications: Review and future potential,” *Sol. Energy Mater. Sol. Cells* **161**, 285–266 (2017).
- 92 I. Čelanović, F. O’Sullivan, M. Ilak, *et al.*, “Design and optimization of one-dimensional photonic crystals for thermophotovoltaic applications,” *Optics Letters* **29**(8), 863–865 (2004).
- 93 M. Modest, *Radiative heat transfer*, Oxford : Academic, 3 ed. (2013).
- 94 Y. Yeng, *Photonic Crystals for High Temperature Applications*. PhD thesis, Massachusetts Institute of Technology (2014).
- 95 V. Stelmakh, V. Rinnerbauer, W. Chan, *et al.*, “Performance of tantalum-tungsten alloy selective emitters in thermophotovoltaic systems,” *Proc. of SPIE* **9115**, 911504–1–8 (2014).
- 96 C. Schlemmer, J. Aschaber, V. Boerner, *et al.*, “Thermal stability of micro-structured selective tungsten emitters,” *AIP Conference Proceedings* **653**, 164–173 (2003).
- 97 N. R. Denny, S. E. Han, D. J. Norris, *et al.*, “Effects of thermal processes on the structure of monolithic tungsten and tungsten alloy photonic crystals,” *Chem. Mater.* **19**, 4563–4569 (2007).

- 98 N. R. Denny, F. Li, D. J. Norris, *et al.*, “In situ high temperature TEM analysis of sintering in nanostructured tungsten and tungsten molybdenum alloy photonic crystals,” *J. Mater. Chem.* **20**(8), 1538–1545 (2010).
- 99 S. G. Rudisill, Z. Wang, and A. Stein, “Maintaining the structure of templated porous materials for reactive and high-temperature applications,” *Langmuir* **28**, 7310–7324 (2012).
- 100 H. J. Lee, K. Smyth, S. Bathurst, *et al.*, “Hafnia-plugged microcavities for thermal stability of selective emitters,” *Appl. Phys. Lett.* **102**(24) (2013).
- 101 U. Guler, A. Boltasseva, and V. Shalaev, “Refractory plasmonics,” *Science* **344**, 263–264 (2014).
- 102 V. Rinnerbauer, Y. Yeng, W. Chan, *et al.*, “High-temperature stability and selective thermal emission of polycrystalline tantalum photonic crystals,” *Opt. Express* **21**(9), 11482–11491 (2013).
- 103 V. Stelmakh, D. Peykov, W. R. Chan, *et al.*, “Thick sputtered tantalum coatings for high-temperature energy conversion applications,” *Journal of Vacuum Science and Technology A: Vacuum, Surfaces, and Films* **33**, 061204 (2015).
- 104 V. Stelmakh, V. Rinnerbauer, R. Geil, *et al.*, “High-temperature tantalum tungsten alloy photonic crystals: Stability, optical properties, and fabrication,” *Appl. Phys. Lett.* **103**, 123903 (2013).
- 105 P. Nagpal, D. Josephson, N. Denny, *et al.*, “Fabrication of carbon / refractory metal nanocomposites as thermally stable metallic photonic crystals,” *J. Mater. Chem.* **21**, 10836 (2011).
- 106 D. Peykov, Y. X. Yeng, I. Čelanović, *et al.*, “Effects of surface diffusion on high temperature selective emitters,” *Opt. Express* **23**(8), 9979 (2015).

- 107 M. Shimizu, A. Kohiyama, and H. Yugami, “Evaluation of thermal stability in spectrally selective few-layer metallo-dielectric structures for solar thermophotovoltaics,” *J. Quant. Spectrosc. Radiat. Transfer* **212**, 45–49 (2018).
- 108 R. Nelson, “A brief history of thermophotovoltaic development,” *Semicond. Sci. Technol.* **18**, S141 (2003).
- 109 B. Bitnar, W. Durisch, and R. Holzner, “Thermophotovoltaics on the move to applications,” *Applied Energy* **105**, 430–438 (2013).
- 110 Tektronix, *Lithium-Ion Battery Maintenance Guidelines*.

List of Figures

- 1 The basic three components of a TPV system are a heat source, an emitter, and a photovoltaic (PV) cell (sometimes the PV cell is known as the TPV cell). The hot side is made up of a heat source in thermal contact with an emitter and converts heat to light. On the cold side, the PV cell converts the thermal radiation from the emitter into electricity. Sometimes the cold side includes a front side filter or back surface reflector, to be explained later. A near-field TPV device has a subwavelength gap between the emitter and the PV cell, but we only focus on standard TPV systems.

- 2 Three categories of TPV emitters include those that have been i) used in published system demonstrations of TPV prototypes ii) fabricated and measured and iii) simulated. The emitters in this figure emit in approximately 1-3 μm range. Abbreviations and some terminology: atomic symbols are used, ARC is an anti-reflection coating, a photonic crystal is a periodic structure,⁴ and a metamaterial is a manmade material that has optical properties not usually found in nature, metasurfaces are a class of metamaterials that consist of a 2D array of metal features on a dielectric spacer on a metal substrate.
- 3 The proposed five metrics for practical TPV emitters include 1) optical performance 2) ability to scale to large areas 3) long-term high-temperature stability 4) ease of integration within the TPV system and 5) cost. Each has sub-metrics as shown.
- 4 An emitter with good optical performance may have a) either broadband emission, where any in-band photons (energy greater or wavelength shorter than the PV cell bandgap, where E_{PV} and λ_{PV} are the bandgap energy and wavelength respectively) are preferentially emitted, or narrow-band emission, where only photons with energy slightly above the bandgap are emitted. Note that we refer to photons or radiation both in terms of energy and wavelength. b) The goal of angular control is to ensure good spectral control (preferential in-band emission) over a wide range of angles, as thermal radiation can be off-normal. c) View factor loss, where photons are lost through the emitter-PV cell gap, is a significant source of loss.

List of Tables

- 1 A few (this list is not exhaustive) studies of high-temperature stability of TPV emitters.
- 2 At-a-glance summary of prototype TPV system demonstrations. PhC = photonic crystal.
- 3 Details on prototype TPV system demonstrations, part I. Bulk emitters: Si, SiC, metals with and without anti-reflection coating (ARC). D = diameter, L = length.
- 4 Details on prototype TPV system demonstrations, part II. Naturally selective emitters based on rare earth materials, 1D photonic crystals, 2D photonic crystals. D = diameter, L = length.
- 5 Details on prototype TPV system demonstrations, part III. Multilayer stacks. D = diameter, L = length.

A Evaluation of emitters used in published system demonstrations of prototype TPV

Because there is no consistency in the optical performance figures of merit reported by papers, we have used the following methods to find or calculate $M_{\text{rad,in}}$ (or P) and $\eta_{\text{ri-input}}$:

1. Reported the numerical values for power provided in the paper
 - (a) $P_{\text{rad,in}}$ or $P_{\text{rad,out}}$
 - (b) $P_{\text{total, in-band}}$
2. Calculation is based on radiation spectrum (power density as a function of photon energy)
 - (a) Radiation spectrum at high temperature
 - (b) Radiation spectrum at unknown or room temperature

3. Calculation is based on the measured or simulated spectrum of emittance or absorptance, emitter temperature T_{emitter} , and PV cell bandgap or cutoff
 - (a) Hemispherical emittance spectrum at $T \sim T_{\text{emitter}}$
 - (b) Hemispherical emittance spectrum at a temperature that is unknown or not close to T_{emitter}
 - (c) Emittance at a single or unknown angle, at $T \sim T_{\text{emitter}}$
 - (d) Absorptance at a single or unknown angle, at a temperature that is not close to T_{emitter}
 - (e) Emittance at a single or unknown angle, at a temperature that is unknown or not close to T_{emitter}
4. Calculation is based on assumption of greybody emitter behavior with $\varepsilon' = 0.96$ unless otherwise stated in the paper, ignoring any effects of a cold side filter if included
5. No calculation
 - (a) T_{emitter} or emitter temperature range is provided, but no emittance spectrum is provided
 - (b) Neither emittance nor T_{emitter} are provided

Emitter	Cutoff $\mu\text{m}/$ (eV)	T_{emitter} (K)	$M_{\text{rad,in}}$ (W cm^{-2})	$P_{\text{rad,in}}$ (W)	P_{input} (W)	$\eta_{\text{ri-input}}$	Method	Area	High temp. studies	Vacuum/ inert?	Emitter fab. w/ heat src?
Si ⁶	2.27 (0.547)	~1013	0.688	0.688	13.7	0.0502	4	10 mm x 10 mm	-	Yes	Yes
Si _x N _y -coated Si ⁵	1.72	1043	0.183	-	1.3	-	3b	-	-	-	Yes
SiC, with filter ⁷	1.8	-	-	-	-	-	5b	D 1.5 in., L 3.5 in.	-	-	-
Double-chambered SiC cylinder, with filter ⁸	1.7	1053	-	1.62; 0.246 W transmit. through filter	497	0.0326	1a	-	-	-	Yes
Commercial SiC radiant burner ^{9,10}	1.8	1323	2.28	-	-	-	4	-	-	-	Yes
SiC, with filter ¹¹	2.07 (0.6)	1312	3.37	98.3	-	-	4	5.4 cm x 5.4 cm	-	-	-
Combined emitter- combustor: SiC ¹²	1.8	1120	0.593	-	-	-	4	-	-	-	Yes
ARC on W on SiC ¹³	1.8	1548	5.2	2439	-	-	1a	469 cm ² , cylindrical	-	-	-
ARC-coated Pt foil ¹⁴	1.8	1287	-	69	497	0.0994	1a	>38 cm ²	-	Designed for inert gas	-
Same as above, different test condition	1.8	1287	-	142	952	0.149	1a	>38 cm ²	-	Designed for inert gas	-
HfO ₂ -coated W foil ¹⁵	1.88	1300- 1500	-	-	-	-	5a	D 12 mm, L 25 mm	-	Ar flow	-
Absorber/emitter: Si ₃ N ₄ -coated, laser-textured W ¹⁶	1.8 (0.67)	1456	2.74	17.1	68.8	0.249	3e	Absorber: 7.7 mm x 7.7 mm, Emitter: 25 mm x 25 mm	-	<10 mTorr	-
W-coated SiSiC cylinder ¹⁷	1.8	1463	-	-	1800	-	5a	D 55 mm L >50 mm	-	Ar >20 mbar	Yes
Combined emitter- combustor: Pt ¹²	1.8	1450	0.362	-	-	-	3e	-	-	-	Yes
Burner made of unspecified "super alloy" ¹⁹	1.73 (0.72)	1458	-	5.86	11.77 kW	0.250	1b	D 8.0 cm, L 25.5 cm; effective emitter area: 502 cm ²	-	-	Yes
Absorber/ Emitter: W (Ta?) foil cylinder ¹⁸	1.82	1720	8.90	0.60	64.8; (180 W m ⁻²)	0.0093	3d	Concentrator: 0.6 m x 0.6 m, Emitter: D 12 mm, L 15 mm	-	-	-
Same as above, but longer cylinder ¹⁸	1.82	1400	2.31	0.47	64.8; (180 W m ⁻²)	0.0072	3d	Concentrator: 0.6 m x 0.6 m, Emitter: D 12 mm, L 45 mm	-	-	-

Table 3 Details on prototype TPV system demonstrations, part I. Bulk emitters: Si, SiC, metals with and without anti-reflection coating (ARC). D = diameter, L = length.

Emitter	Cutoff $\mu\text{m}/$ (eV)	T_{emitter} (K)	$M_{\text{rad,in}}$ (W cm^{-2})	$P_{\text{rad,in}}$ (W)	P_{input} (W)	$\eta_{\text{ri-input}}$	Method	Area	High temp. studies	Vacuum/ inert?	Emitter fab. w/ heat src?
Gas mantle in a commercial camping lantern ^{20,108}	1.1 (1.1)	1570- 1970	-	-	-	-	5a	-	-	-	-
Absorber/emitter: SiC plate, Emitter: single crystal Er doped yttrium aluminum garnet ²¹	1.1, 1.65	1133- 1473	-	-	1006 kW m^{-2}	-	5a	-	Post 300 hours in sun, emitter cracked & darkened, but may be due to water leak ²¹	-	-
$\text{Al}_2\text{O}_3/\text{Er}_3\text{Al}_5\text{O}_{12}$ composite, w/ polished Mo pinhole outside emitter ²²	1.8	1254	0.634	0.63	100- 450	0.0014- 0.0063	3e	10 mm x 10 mm	-	-	-
Yb_2O_3 mantle, w/ filter ²³	1.1	-	-	-	11723	-	5b	D 1.5 in., L 8 in.	-	-	-
Yb_2O_3 fibrous mantle ²⁶	1.1	-	-	-	-	-	5b	-	-	-	-
Yb_2O_3 mantle ^{24,25}	1.1 (1.1)	1735	1.32	71.1	2000	0.0356	2b	Actual 75 cm^2 , Effective 54 cm^2	-	-	-
Yb_2O_3 -coated Al_2O_3 or SiC foam ceramic ^{25,109}	1.1 (1.1)	~ 1735	1.27	-	-	-	2b	-	200 thermal cycles ²⁵	-	-
1D photonic crystal (PhC), 5 alternating layers of Si, SiO_2 directly deposited on Si microreactor ⁶	2.27 (0.457)	~ 1073	0.584	0.584	13.7	0.0426	2a	10 mm x 10 mm	-	Yes	Yes
Absorber: vertically aligned multiwall carbon nanotubes, Emitter: 1D PhC of Si, SiO_2 on Si ²⁷	2.25 (0.55)	1285	3.44	3.44	16 (48 W cm^{-2})	0.215	3c	Absorber 0.1 cm^2 , emitter: 1 cm^2	-	< 0.5 Pa	Yes
As above, absorber: carbon nanotubes, Emitter: 1D Si/ SiO_2 PhC; w/ cold side rugate filter ²⁸	2.25 (0.55)	-	-	-	-	-	5b	Emitter: 4 cm^2 , 2 ratios $A_{\text{emitter}}/$ A_{absorber} : 12 and 7, Filter: 4 cm^2	-	< 0.5 Pa	Yes
Absorber & emitter each: 2D photonic crystal made of polycrystalline Ta w/ HfO_2 coating ²⁹	2.3 (0.54)	1270	1.37	-	130 kW m^{-2} (130 suns), if A_a $= A_e$	0.106	3a	-	1 hour at 1000 $^\circ\text{C}$, 144 hours at 900 $^\circ\text{C}$ ¹⁰²	< 0.3 Pa	-
2D photonic crystal made of polycrystalline Ta w/ HfO_2 coating ³⁰	2.0	1327	4.08	18	100	0.18	1a & 3b	~ 21 mm x 21 mm	> 100 hours at 900 $^\circ\text{C}$, no degra- dation in structure or optical perf. ³⁰	Yes	No
2D photonic crystal made of Ta3%W alloy w/ HfO_2 coating ^{31,32}	2.25 (0.55)	1233	2.01	2.01	53	0.0379	1b & 3d	1 cm x 1 cm	300 hours at 1000 $^\circ\text{C}$, ¹ 1 hour at 1200 $^\circ\text{C}$ ¹⁰⁴	1×10^{-5} Torr	No

Table 4 Details on prototype TPV system demonstrations, part II. Naturally selective emitters based on rare earth materials, 1D photonic crystals, 2D photonic crystals. D = diameter, L = length.

Emitter	Cutoff $\mu\text{m}/$ (eV)	T_{emitter} (K)	$M_{\text{rad.in}}$ (W cm^{-2})	$P_{\text{rad.in}}$ (W)	P_{input} (W)	$\eta_{\text{ri-input}}$	Method	Area	High temp. studies	Vacuum/ inert?	Emitter fab. w/ heat src?
Combined emitter absorber: multilayer stack w/ subwavelength layers of W, yttria- stabilized zirconia ³³	1.85 (0.67)	1640	9.79	17.3	79	0.219	3e	Absorber D: 15 mm, Emitter D: 15 mm	-	1.0×10^{-5} Pa	Yes
Combined emitter absorber: multilayer stack w/ subwavelength layers of Mo, HfO ₂ ³⁴	1.85 (0.67)	1640	6.62	4.21	0.260	16.2	3b	Absorber D: Pa, 6 mm, Emitter D: 9 mm	No degrad. post 1 hour at 1423 K, $<5 \times 10^{-2}$ 2 rapid thermal cycles 500-1250 K, but degrad. post 1 hour at 1473 K ¹⁰⁷	4.6×10^{-3} Pa	Yes

Table 5 Details on prototype TPV system demonstrations, part III. Multilayer stacks. D = diameter, L = length.